Computers & Structures Vol. 39, No. 5, pp. 473–482, 1991
Printed in Great Britain.

0045-7949/91 $3.00 + 0.00
© 1991 Pergamon Press plc

DYNAMIC ANALYSIS OF FLEXIBLE STRIP-FOUNDATIONS IN THE FREQUENCY DOMAIN†

F. T. KOKKINOS and C. C. SPYRAKOS
Department of Civil Engineering, West Virginia University, Morgantown, WV 26506-6101, U.S.A.

(*Received* 26 *March* 1990)

Abstract—This work deals with the development and presentation of a frequency domain hybrid numerical method for determining the dynamic response of surface strip-foundations under conditions of plane strain placed on an elastic soil medium and subjected to either externally applied forces or seismic disturbances. The elastic, isotropic, and homogeneous soil medium is treated with the boundary element method, while the flexible and massive foundation is treated with the finite element method. The two methods are appropriately combined through equilibrium and compatibility conditions at the soil foundation interface. Several numerical examples are worked out to demonstrate and attest the efficiency and accuracy of the method.

1. INTRODUCTION

In recent years, the dynamic response of two and three-dimensional footings placed on a linear elastic half-space and subjected to external dynamic loads has been investigated extensively. The loads may be either a harmonic force excitation, as in the case of machine foundations, or a seismic load (specified either as base acceleration or prescribed free field displacements) represented by their frequency content. In these cases the analyses are performed preferably in the frequency domain. Furthermore, under these loading conditions, the analysis and design must account for the interaction between the foundation and the soil, since the soil-foundation interface moves or distorts differently from the corresponding surface in the free field. The response of the structure–foundation system is influenced by the soil which exhibits an essential feature, the geometric damping. This is due to the fact that waves travel out to infinity resulting in energy dissipation even if the soil is assumed to consist of a purely elastic material.

Several computational procedures are presently available to obtain dynamic impedance functions and the foundation response for each specific problem [1]. In boundary value problems, the boundary element method (BEM) presents several advantages over domain methods when analyzing viscoelastic homogeneous media with a large volume-to-surface ratio. Such advantages include reduction of the problem dimensionality by one, consideration of the radiation condition at infinity and enhancement of numerical accuracy [2]. The BEM has been applied to the general soil structure interaction (SSI) area of research through either a frequency or a time domain formulation. Cruze and Rizzo [3] presented a frequency domain BEM formulation of general two- and three-dimensional elastodynamic problems. Niwa *et al.* [4] and Banaugh and Goldsmith [5] applied a frequency domain BEM to study steady-state wave propagation problems. Ottenstreuer and Schmid [6] studied the problem of cross-interaction between two rigid surface foundations. Antes and v. Estorff [7] presented time-dependent BE procedures to treat general two-dimensional elastodynamic problems under arbitrary initial conditions and body forces. Antes' research was restricted to rigid-type foundations.

The versatility and accuracy of the finite element method (FEM) in analyzing finite domains is well established [8, 9]. In treating SSI problems, however, FEM poses distinct disadvantages over BEM, stemming from its inability to appropriately model semi-infinite soil media [10, 11]. In order to take advantage of the merits of both methods, it is preferable to treat the finite size structure with the FEM, the supporting semi-infinite soil with the BEM and combine the two methods through appropriate equilibrium and compatability conditions at the soil-foundation interface. Adopting a hybrid approach, analysis and design are not restricted to simple-geometry structures or undamped systems, but can be extended to composite structures, multiply-connected structural systems and also account for viscous or hysteretic damping [12–18].

Several authors have studied the problem of obliquely incident waves impinging on a rigid or flexible foundation. Wong and Luco [19] were the first to study the dynamic response of a rigid massless rectangular foundation, while Whittaker and Christiano [20] studied the case of flexible surface foundations. Dominguez [21] applied a frequency domain BEM to the study of rigid massless foundations and

† Portions of this work have been presented at the 2nd National Congress on Mechanics of the Hellenic Society for Theoretical and Applied Mechanics (HSTAM), Athens, June 1989.

Antes and Spyrakos [22] analyzed the response of massive blocks to transient Rayleigh waves using the time domain BEM.

In this work two separate formulations are presented in order to study the cases of externally applied harmonic loads and harmonic seismic wave excitations. The salient features of the frequency domain BEM–FEM are compared with approximations commonly adopted by analytical/numerical approaches or purely numerical FEM methods. Parametric studies examining the effect of the relative stiffness and relative mass between the foundation and the soil, and the spatial distribution of the dynamic disturbances on the foundation response are presented. The work at hand is one of the initial attempts to investigate the dynamic behavior of strip-plates accounting for both the foundation flexibility and inertia [23].

2. FORMULATION AND NUMERICAL IMPLEMENTATION

The sequence of presenting the hybrid BEM–FEM formulation, as can be applied to elastodynamic problems, consists of three steps. Namely, the development of an integral equation corresponding to Navier–Cauchy equations and boundary conditions of an infinite linear elastic or viscoelastic medium; the development of the differential equations and boundary-initial conditions associated with the finite domain; and the numerical treatment of the governing integral and differential equations with the aid of the BEM and FEM, respectively. Herein the infinite medium is the soil, while the system of finite dimensions is the overlaying foundation, as shown in Fig. 1.

2.1. *Basic theory*

Consider a homogeneous isotropic and linear elastic body R with boundary S subjected to body forces $\bar{\mathbf{b}}(\mathbf{x}; t)$. In steady-state elastodynamics the displacement vector associated with each point $\mathbf{x} \in R + S$ is given by $\tilde{\mathbf{u}}(\mathbf{x}; t) = \mathbf{u}(\mathbf{x}; \omega)e^{i\omega t}$. Under the assumption of small displacement theory and for plane strain conditions, the elastodynamic displacement field of body R is governed by Navier's equation of equilibrium [24],

$$(c_1^2 - c_2^2)u_{j,ji} + c_2^2 u_{i,jj} + \frac{b_i}{\rho_s} = k^2 u_i - k u_{0i} - v_{0i} \quad (i, j = 1, 2), \quad (1)$$

where $k = i\omega (i = \sqrt{-1})$, ω is the circular frequency of the problem, $u_{0i}(\mathbf{x})$ and $v_{0i}(\mathbf{x})$ are the initial displacement and velocity, respectively, and $\bar{b}_i(\mathbf{x}; k)$ are the Laplace transforms of $\tilde{b}_i(\mathbf{x}; t)$, which are the components of the body force per unit volume. In the above equation, c_1 and c_2 are the dilatational and shear complex wave velocities, respectively, given in terms of the modulus of elasticity E_s, Poisson's ratio ν_s and mass density ρ_s by,

$$c_1 = \sqrt{\frac{E_s(1 + 2\zeta_1 i)(1 - \nu_s)}{\rho_s(1 + \nu_s)(1 - 2\nu_s)}}$$

and

$$c_2 = \sqrt{\frac{E_s(1 + 2\zeta_2 i)}{2\rho_s(1 + \nu_s)}}, \quad (2)$$

where the subscript s indicates that the elastic constants refer to the soil. In eqn (2), ζ_1 and ζ_2 denote the ratios of the linear hysteretic damping for P- and S-waves, respectively. Linear hysteretic damping is independent of the frequency of excitation, ω, and can be introduced into the solution, when working in the frequency domain, by using the correspondence principle [25]. The latter states that the damped solution is obtained from the elastic one by replacing the elastic constants by the corresponding complex ones. Hysteretic damping does not fulfil the causality requirement, a necessary condition to apply the correspondence principle. Nevertheless, its use leads to reasonably accurate results for very deep soil deposits and halfspace soil idealizations [1, 26]. In the present work it is assumed that the damping coefficients for the two waves are equal, which implies that the Poisson's ratio is real, and ζ_s will refer to the soil, while ζ_f to the strip-foundation.

For the general case we have to consider a mixed boundary value problem with boundary conditions,

$$\alpha(\mathbf{x})u_i(\mathbf{x}; k) + \beta(\mathbf{x})t_i(\mathbf{x}; k) = \gamma(\mathbf{x}), \quad \mathbf{x} \in S_\beta \quad (3)$$

$$u_i(\mathbf{x}; k) \to 0 \quad \text{and} \quad t_i(\mathbf{x}; k) \to 0, \quad \mathbf{x} \in S_\infty, \quad (4)$$

where $S = S_\beta \cup S_\infty$, as shown in Fig. 1; $\alpha(\mathbf{x})$, $\beta(\mathbf{x})$, $\gamma(\mathbf{x})$ are known functions on S_β, and $t_i(\mathbf{x}; k)$ are the traction components on the boundary. It must be pointed out that condition (4) is valid only

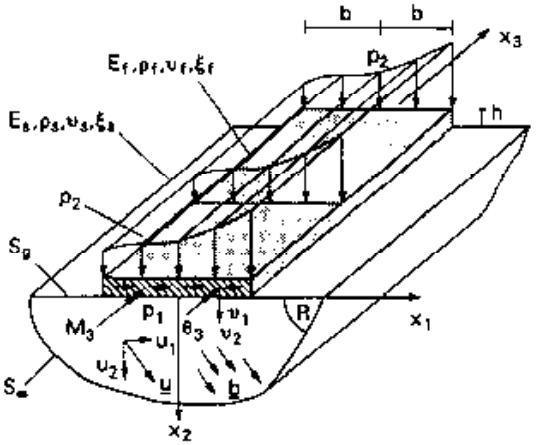

Fig. 1. Geometry, loading and material constants of the soil–foundation system.

when the domain R extends to infinity in the half-plane. The solution of eqn (1) is given by the following integral representation [27],

$$\tfrac{1}{2}u_i(Q;k) = \int_{S_R} t_j(P;k)U_{ij}(P,Q;k)\,dS(P) - \int_{S_R} u_j(P;k)T_{ij}(P,Q;k)\,dS(P) + \iint_R \left(\frac{b_j(p;k)}{\rho_r} + ku_{0j}(p) + v_{0j}(p)\right) \times U_{ij}(p,Q;k)\,dA(p), \quad (5)$$

where $dA(p)$ is an area element at a field point $p(\mathbf{x}) \in R$ and $dS(P)$ is an element on the boundary at a field point $P(\mathbf{x}) \in S$. The arguments of elements dA and dS denote the point which varies during integration. The fundamental solutions $U_{ij}(p(\mathbf{x}), q(\xi); k)$ and $T_{ij}(p(\mathbf{x}), q(\xi); k)$ express displacement and traction components, respectively, in the x_j-direction at the observation point $p(\mathbf{x})$ at a distance $r = |\mathbf{x} - \xi|$ away from the source point $q(\xi)$, due to a concentrated unit load acting at $q(\xi)$ in the x_i-direction. The two-point tensors U_{ij} and T_{ij} are given explicitly by the following formulae [24]

$$U_{ij}(\mathbf{x},\xi;k) = \frac{1}{2\pi\rho_r c_2^2}(\bar{\psi}\delta_{ij} - \bar{\chi}r_{,i}r_{,j}) \quad (6)$$

$$T_{ij}(\mathbf{x},\xi;k) = \frac{1}{2\pi}\left[\left(\frac{d\bar{\psi}}{dr} - \frac{\bar{\chi}}{r}\right)\left(\delta_{ij}\frac{\partial r}{\partial \eta} + r_{,j}n_i\right) - 2\frac{\bar{\chi}}{r}\left(n_j r_{,i} - 2r_{,i}r_{,j}\frac{\partial r}{\partial \eta}\right) - 2\frac{d\bar{\chi}}{dr}r_{,i}r_{,j}\frac{\partial r}{\partial \eta} + \left(\frac{c_2^2}{c_2^2} - 2\right)\left(\frac{d\bar{\psi}}{dr} - \frac{d\bar{\chi}}{dr} - \frac{\bar{\chi}}{r}\right)r_{,i}n_j\right], \quad (7)$$

where

$$\bar{\psi} = K_0\left(\frac{kr}{c_2}\right) + \frac{c_2}{kr}\left[K_1\left(\frac{kr}{c_2}\right) - \frac{c_2}{c_1}K_1\left(\frac{kr}{c_1}\right)\right], \quad (8)$$

$$\bar{\chi} = K_2\left(\frac{kr}{c_2}\right) - \left(\frac{c_2}{c_1}\right)^2 K_2\left(\frac{kr}{c_1}\right), \quad (9)$$

and

$$r = [(x_i - \xi_i)(x_i - \xi_i)]^{1/2} \quad (i = 1, 2). \quad (10)$$

In eqns (8) and (9), $K_0(z)$, $K_1(z)$, $J_2(z)(z \in \mathcal{S})$ are modified zero-, first- and second-order Bessel functions of the second kind, respectively. Definitions and properties of the modified Bessel functions K_i $(i = 0, 1, 2)$ can be found in various sources, e.g. [28, 29]. Equation (5) can be viewed as a constraint equation between the transformed traction vector and displacement vector on the boundary and the transformed body force in the interior of the body.

The second constituent of the soil–structure system is a massive flexible strip-foundation in complete bond with the soil. On the basis of the Bernoulli–Euler beam theory, the axial and flexural motions of a unit width of the strip-foundation are governed by the following uncoupled equations [27]

$$\bar{E}_f h v_1'' + \rho_f h\omega^2 v_1 = -(p_1 - \tau_{21}) \quad (11)$$

and

$$\bar{D}_f v_2'''' - \rho_f h\omega^2 v_2 = p_2 - \tau_{22}. \quad (12)$$

where $v_1 = v_1(x_1; k)$ and $v_2 = v_2(x_1; k)$ are the amplitudes of the axial and the flexural motion, respectively. In the above equation $p_1(x_1; k)$ and $p_2(x_1; k)$ are the amplitudes of the externally applied harmonic forces, while $\tau_{21}(x_1; k)$ and $\tau_{22}(x_1; k)$ are the contact stresses applied on a unit width of the foundation. According to the correspondence principle [25], material damping has been taken into account by introducing the complex modulus of elasticity, $\bar{E}_f = E_f(1 + 2\zeta_f i)$ and the complex flexural rigidity, $\bar{D}_f = \bar{E}_f h^3/12(1 - \nu_f^2)$, with h, ν_f and ζ_f denoting the thickness, the Poisson's ratio and the damping coefficient of the linearly elastic foundation, respectively. Evaluation of the flexible foundation response can be obtained by numerical solution of the system of eqns (5), (11) and (12) with the associated boundary and initial conditions.

2.2. *Numerical treatment*

In this investigation the boundary integral eqn (5) can be discretized by dividing the boundary $S_R = S_f \cup S_c$ of the soil surface into an $M = M_f + M_c$ number of boundary elements. The soil–foundation contact area S_c is divided into M_c elements, while the free soil surface S_f is divided into M_f elements, as shown in Fig. 2. The elements are not necessarily equal, they are numbered consecutively from left to

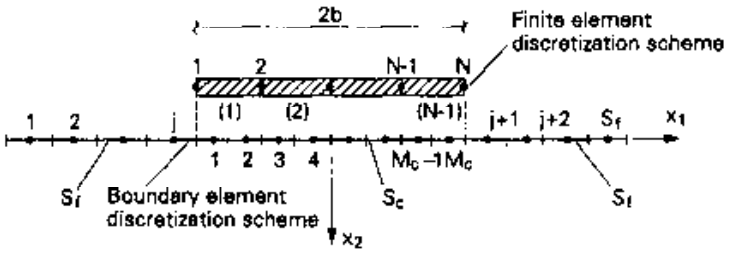

Fig. 2. Typical BEM–FEM discretization.

right and the nodal points are placed at the center of the corresponding boundary elements. The values of the boundary displacements u_i and tractions t_i $(i = 1, 2)$ are assumed constant over each element (step function assumption) and equal to their values at the nodal point of the element.

Under the assumption of zero body forces and initial conditions, eqn (5) can be written in the following form.

$$\tfrac{1}{2}\{u\}_m = \sum_{n=1}^{M} [G]_{mn}\{t\}_n - \sum_{n=1}^{M} [H]_{mn}\{u\}_n \qquad (13)$$

where $m, n = 1, 2, 3, \ldots, M$,

$$\{u\}_m = \begin{Bmatrix} u_1(\xi_m; k) \\ u_2(\xi_m; k) \end{Bmatrix}, \quad \{t\}_n = \begin{Bmatrix} t_1(\mathbf{x}_n; k) \\ t_2(\mathbf{x}_n; k) \end{Bmatrix},$$

$$\{u\}_n = \begin{Bmatrix} u_1(\mathbf{x}_n; k) \\ u_2(\mathbf{x}_n; k) \end{Bmatrix}$$

and

$$[G]_{mn} = \begin{bmatrix} \int_n U_{11}(\mathbf{x}, \xi_m; k)\, dS(\mathbf{x}) & \int_n U_{12}(\mathbf{x}, \xi_m; k)\, dS(\mathbf{x}) \\ \int_n U_{21}(\mathbf{x}, \xi_m; k)\, dS(\mathbf{x}) & \int_n U_{22}(\mathbf{x}, \xi_m; k)\, dS(\mathbf{x}) \end{bmatrix}, \qquad (14)$$

$$[H]_{mn} = \begin{bmatrix} \int_n T_{11}(\mathbf{x}, \xi_m; k)\, dS(\mathbf{x}) & \int_n T_{12}(\mathbf{x}, \xi_m; k)\, dS(\mathbf{x}) \\ \int_n T_{21}(\mathbf{x}, \xi_m; k)\, dS(\mathbf{x}) & \int_n T_{22}(\mathbf{x}, \xi_m; k)\, dS(\mathbf{x}) \end{bmatrix}, \qquad (15)$$

In the above equations ξ_m denotes the spatial vector of node m, where the solution point is positioned and $\mathbf{x}_n$ is the spatial vector of the variable node n. The integration point $\mathbf{x}$ in eqns (14) and (15) varies along the n element and when $m \neq n (r \neq 0)$ the line integrals are regular and can be evaluated using any of the known numerical techniques for the evaluation of line integrals. However, when $m = n$ the argument r vanishes when $\mathbf{x} \equiv \xi$ and the values of the singular integrals are established by a limiting process for $r \to 0$. In this investigation these line integrals are computed using the technique presented in [27].

Equation (13) can be written for every boundary element $m = 1, 2, 3, \ldots, M$, in which case the resulting system of $2M$ simultaneous linear algebraic equations can be cast in a matrix form as

$$[\hat{H}]\{u\} - [G]\{t\} = \{0\}, \qquad (16)$$

where $[\hat{H}] = [H] + \frac{1}{2}[I]$, and the entries of the $(2M \times 2M)$ matrices $[H]$ and $[G]$ are given in eqns (14) and (15), respectively. Furthermore, eqn (16) can be rewritten in the following partitioned form as

$$\begin{bmatrix} [\hat{H}_{cc}] & [\hat{H}_{cf}] \\ [\hat{H}_{fc}] & [\hat{H}_{ff}] \end{bmatrix} \begin{Bmatrix} \{u_c\}_{(2M_c \times 1)} \\ \{u_f\}_{(2M_f \times 1)} \end{Bmatrix} = \begin{bmatrix} [G_{cc}] & [G_{cf}] \\ [G_{fc}] & [G_{ff}] \end{bmatrix} \begin{Bmatrix} \{t_c\}_{(2M_c \times 1)} \\ \{t_f\}_{(2M_f \times 1)} \end{Bmatrix}, \qquad (17)$$

where the subscripts c and f designate elements on the soil–foundation contact surface and on the free surface, respectively. Applying the boundary condition $\{t_f\} = \{0\}$, i.e. the part S_f of the soil surface is traction free, in eqn (17), one can easily eliminate the free-surface displacements and obtain a stiffness equation of the form

$$\{t_c\} = [S]_{(2M_c \times 2M_c)}\{u_c\}, \qquad (18)$$

where

$$[S] = ([G_{cc}] - [\hat{H}_{cf}][\hat{H}_{ff}]^{-1}[G_{fc}])^{-1} \times ([\hat{H}_{cc}] - [\hat{H}_{cf}][\hat{H}_{ff}]^{-1}[\hat{H}_{fc}]). \qquad (19)$$

In the above equations ξ_m denotes the spatial vector of node m, where the solution point is positioned and $\mathbf{x}_n$ is the spatial vector of the variable node n. The integration point $\mathbf{x}$ in eqns (14) and (15) varies along the n element and when $m \neq n (r \neq 0)$ the line integrals are regular and can be evaluated using any of the known numerical techniques for the evaluation of line integrals. However, when $m = n$ the argument r vanishes when $\mathbf{x} \equiv \xi$ and the values of the singular integrals are established by a limiting process for $r \to 0$. In this investigation these line integrals are computed using the technique presented in [27].

Equation (13) can be written for every boundary element $m = 1, 2, 3, \ldots, M$, in which case the resulting system of $2M$ simultaneous linear algebraic equations can be cast in a matrix form as

$$[\hat{H}]\{u\} - [G]\{t\} = \{0\}, \qquad (16)$$

where $[\hat{H}] = [H] + \frac{1}{2}[I]$, and the entries of the $(2M \times 2M)$ matrices $[H]$ and $[G]$ are given in eqns (14) and (15), respectively. Furthermore, eqn (16) can be rewritten in the following partitioned form as

$$\begin{bmatrix} [\hat{H}_{cc}] & [\hat{H}_{cf}] \\ [\hat{H}_{fc}] & [\hat{H}_{ff}] \end{bmatrix} \begin{Bmatrix} \{u_c\}_{(2M_c \times 1)} \\ \{u_f\}_{(2M_f \times 1)} \end{Bmatrix} = \begin{bmatrix} [G_{cc}] & [G_{cf}] \\ [G_{fc}] & [G_{ff}] \end{bmatrix} \begin{Bmatrix} \{t_c\}_{(2M_c \times 1)} \\ \{t_f\}_{(2M_f \times 1)} \end{Bmatrix}, \qquad (17)$$

where the subscripts c and f designate elements on the soil–foundation contact surface and on the free surface, respectively. Applying the boundary condition $\{t_f\} = \{0\}$, i.e. the part S_f of the soil surface is traction free, in eqn (17), one can easily eliminate the free-surface displacements and obtain a stiffness equation of the form

$$\{t_c\} = [S]_{(2M_c \times 2M_c)}\{u_c\}, \qquad (18)$$

where

$$[S] = ([G_{cc}] - [\hat{H}_{cf}][\hat{H}_{ff}]^{-1}[G_{fc}])^{-1} \times ([\hat{H}_{cc}] - [\hat{H}_{cf}][\hat{H}_{ff}]^{-1}[\hat{H}_{fc}]). \qquad (19)$$

Equation (18) constitutes a system of $2M_c$ equations in $4M_c$ unknowns. The additional $2M_c$ equations which are required to establish the unknown boundary displacements and tractions are derived from the equilibrium and compatibility conditions at the soil–foundation interface and have the general form of eqn (3).

(i) Externally applied loads. The strip-plate dynamic stiffness matrix can be obtained from the expressions presented by Spyrakos and Beskos [30], if the beam rigidity EI is substituted by the strip-plate rigidity $\bar{D}_f$. The advantage of the dynamic stiffness influence coefficients is their ability to capture inertia effects more accurately than conventional finite element procedures using stiffness matrices derived from static FEM formulations. On the assumption that each finite element of the discretized foundation model must be in contact with two successive boundary elements of the supporting soil, the strip-plate is divided into $M_c/2$ finite beam elements (M_c even), introducing in this way $N = M_c/2 + 1$ nodal points. Thus, through standard finite element procedures,

eqns (11) and (12) can be expressed in a partitioned form as

$$\begin{bmatrix}[K_{vv}]_{(2N\times 2M)} & [K_{v\theta}]_{(2N\times M)}\\ [K_{\theta v}]_{(N\times 2M)} & [K_{\theta\theta}]_{(N\times N)}\end{bmatrix}\begin{Bmatrix}\{v\}\\ \{\theta\}\end{Bmatrix} = \begin{Bmatrix}\{P\}\\ \{M\}\end{Bmatrix} - \begin{Bmatrix}\{R\}\\ \{0\}\end{Bmatrix} \tag{20}$$

in which $[K_{vv}]$, $[K_{v\theta}]$, $[K_{\theta v}]$ and $[K_{\theta\theta}]$ are the submatrices of the total dynamic stiffness matrix, $\{v\}$ and $\{\theta\}$ represent the nodal displacement and rotation vectors, $\{P\}$ and $\{M\}$ are the nodal external loads acting on the strip-foundation and $\{R\}$ is the vector of the nodal forces associated with the contact stresses.

Coupling of the matrix eqns (18) and (20) requires correspondence between nodal displacements and tractions as specified by BEM and FEM approximations. In order to introduce compatibility between the deflection of the structure and the soil motion at the interface, the displacement of each node of the finite element discretization scheme is assumed to be equal to the displacements developed over two successive boundary elements joined at this node (Fig. 3a). Similarly, compatibility of forces can be established if each contact force $\{R\}_{(m)}$ $(m = 1, 2, \ldots, N)$ applied at node m of the strip-foundation, is approximated by the resultant of the two forces associated with the contact stresses that develop over the two contiguous elements whose common extreme point coincides with node m (Fig. 3b). Therefore, for the whole interface region, the compatibility conditions can be expressed as

$$\{u_c\} = [C]^T\{v\} \tag{21}$$

and

$$\{R\} = [C][l]\{t_c\}, \tag{22}$$

where the entries of the $(2N \times 2M_c)$ matrix $[C]$ are either 0 or 1, $[l]$ is a $(2M_c \times 2M_c)$ diagonal matrix consisting of the boundary element lengths l_i $(i = 1, 2, \ldots, M_c)$ and the superscript T denotes matrix transposition.

Equations (18) (22) form a system of linear algebraic equations, which can be solved for the unknown displacements $\{v\}$ and rotations $\{\theta\}$ to give

$$\{v\} = ([K_{vv}] - [K_{v\theta}][K_{\theta\theta}]^{-1}[K_{\theta v}] + [C][l][S][C]^T)^{-1} \times (\{P\} - [K_{v\theta}][K_{\theta\theta}]^{-1}\{M\}) \tag{23}$$

and

$$\{\theta\} = [K_{\theta\theta}]^{-1}(\{M\} - [K_{\theta v}]\{v\}). \tag{24}$$

(ii) Obliquely incident seismic waves. Consider now the same foundation in complete bond with the supporting elastic half-space and subjected to seismic waves propagating in a direction parallel to the x_1x_2-plane. By adopting the procedure suggested by Thau [31], the total displacement field $\{u\}$ can be decomposed into two parts: the free field due to the impinging seismic waves, and the scattered field generated by the motion of the foundation in the absence of any seismic excitation. This is expressed mathematically by

$$\{u\} = \begin{Bmatrix}\{u_c\}\\ \{u_f\}\end{Bmatrix} = \begin{Bmatrix}\{u_c^F\}\\ \{u_f^F\}\end{Bmatrix} + \begin{Bmatrix}\{u_c^S\}\\ \{u_f^S\}\end{Bmatrix}, \tag{25}$$

where the superscripts F and S are used to indicate the displacement vectors of the free and scattered fields, respectively. For the displacement amplitudes $\{u_c^F\}$ and $\{u_f^F\}$ of the soil surface, the interaction forces that act at the nodes of the contact area and arise from the soil vanish, as for the free field loading state, the line that will subsequently form the foundation-soil interface is traction free. The interaction forces $\{R\}$ of the soil will thus depend on the scattered field displacements $\{u^S\}$, and according to the equilibrium condition (22) and eqn (28) can be written as

$$\{R\} = [C][l][S][u_f^S], \tag{26}$$

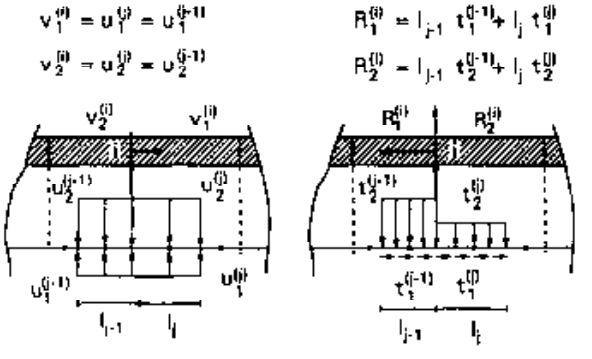

Fig. 3. Coupling conditions at the soil–foundation interface.

where the stiffness matrix $[S]$ of the soil has been defined in eqn (19). Substituting the displacement compatibility condition (21) into the aforegoing eqn (26), a relationship between the interaction forces and the nodal displacements $\{v\}$ is obtained in the form

$$\{R\} = [C][l][S]([C]^T\{v\} - [u_c^F]). \quad (27)$$

For the case of earthquake excitation there are no external loads applied on the strip-foundation and therefore the force–displacement eqn (20) becomes

$$\begin{bmatrix} [K_{vv}]_{(2N\times 2N)} & [K_{v\theta}]_{(2N\times N)} \\ [K_{\theta v}]_{(N\times 2N)} & [K_{\theta\theta}]_{(N\times N)} \end{bmatrix} \begin{Bmatrix} \{v\} \\ \{\theta\} \end{Bmatrix} = - \begin{Bmatrix} \{R\} \\ \{0\} \end{Bmatrix}. \quad (28)$$

The elimination of the rotational degrees of freedom can be achieved by standard condensation operations on the complete dynamic stiffness matrix of eqn (28). Therefore, the reduced stiffness equation can be written as

$$([K_{vv}] - [K_{v\theta}][K_{\theta\theta}]^{-1}[K_{\theta v}])\{v\} = -\{R\}, \quad (29)$$

while the nodal rotations $\{\theta\}$ can be expressed in terms of the nodal displacements according to eqn (24). Finally, direct substitution of eqn (27) into eqn (29) yields the required relationship between the unknown nodal displacements of the strip-foundation and the known seismic excitation at the soil surface. This relationship has the form

$$\{v\} = ([K_{vv}] - [K_{v\theta}][K_{\theta\theta}]^{-1}[K_{\theta v}] + [C][l][S][C]^T)^{-1}[C][l][S]\{u_c^F\}, \quad (30)$$

where the vector $\{u_c^F\}$ denotes the free field displacement amplitudes at the boundary nodal points of the soil–foundation contact area.

3. NUMERICAL RESULTS

A computer program has been written for the numerical evaluation of the dynamic response of strip-foundations subjected either to harmonic loads or seismic waves, by using the numerical procedure described in Sec. 2.2. All calculations have been performed on a VAX 11-785, operating on a VMS 4.1 system with a Fortran compiler.

The first example serves to demonstrate the accuracy and convergence of the proposed method. The rigid strip-foundation of Fig. 4, having width $2b = 5$ ft, mass density $\rho_f = 16.02$ lb sec^2/ft and thickness $h = 0.5$ ft is placed on a linear elastic soil with elastic constants $E_s = 2.58384 \times 10^9$ lb/ft^2, $\nu_s = 0.25$ and mass density $\rho_s = 10.68$ lb sec^2/ft^4. The vertical displacement, horizontal displacement and rocking amplitudes at the midpoint C of the plate are obtained for the three loading cases shown in Fig. 4. The results are compared with those obtained from an analytical/numerical solution [1] for infinitely long

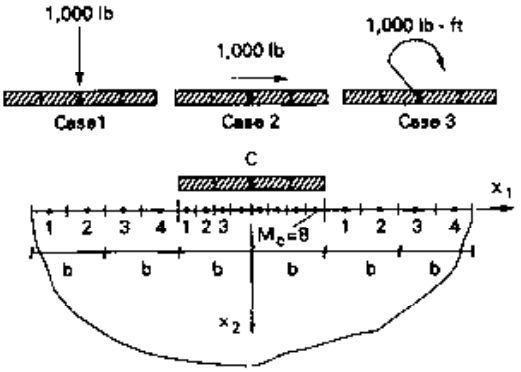

Fig. 4. Discretization and loading of rigid massive strip-foundation.

rigid massive blocks and are presented graphically in Figs. 5–8 vs the dimensionless frequency $\alpha_0 = \omega b/c_2$, ω being the circular frequency of the harmonic loads. For the first two loading cases the results obtained by the BEM–FEM method are in very good agreement with the analytical results. However, the results for concentrated moment at C (Fig. 7) do not compare so well. The difference is attributed to the type of boundary conditions imposed at the soil–foundation interface which do not preserve interelement continuity between the strip-plate elements and the soil surface. In fact for the beam elements, the variation of the displacement function involves hyperbolic functions [30], while a constant variation of the displacement function is assumed for the boundary elements of the soil surface. Thus, as far as rocking is concerned, the model analyzed by the BEM–FEM

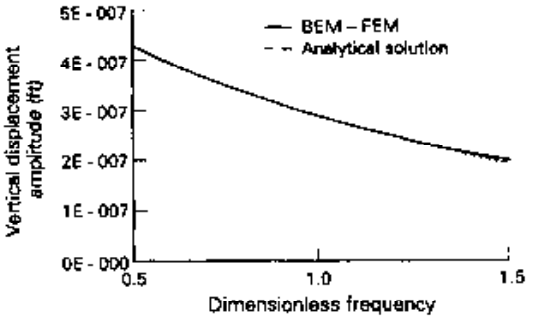

Fig. 5. Vertical response for vertical load at the center.

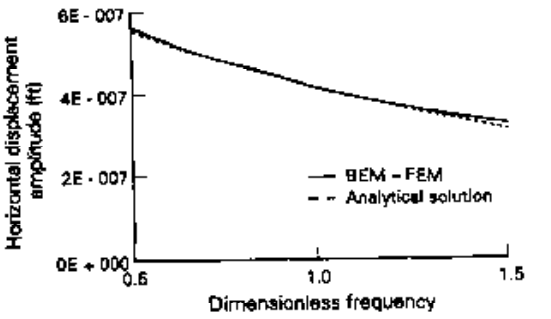

Fig. 6. Horizontal response for horizontal load at the center.

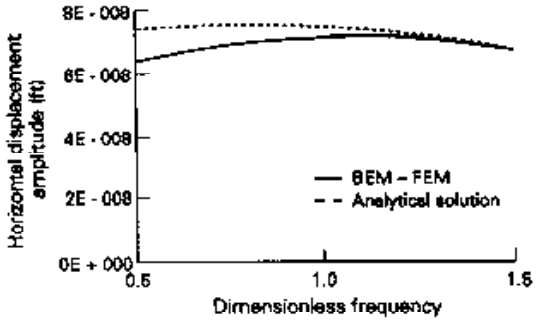

Fig. 7. Horizontal response for concentrated moment at the center.

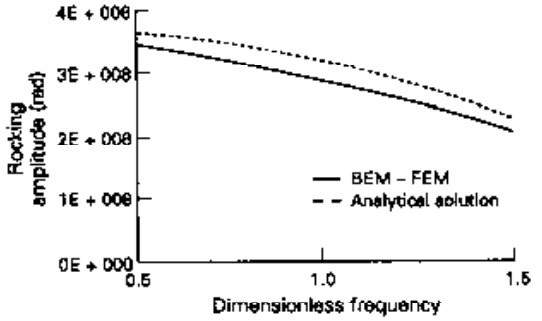

Fig. 8. Rocking amplitude for concentrated moment at the center.

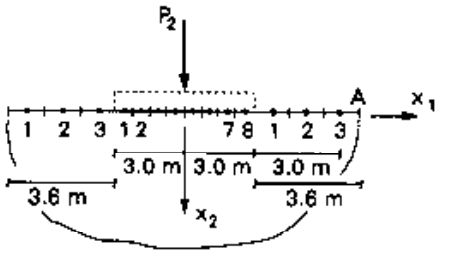

Fig. 10. (a) Discretized soil surface, BEM–FEM modeling ($E_f \approx 0$ and $\rho_f \approx 0$).

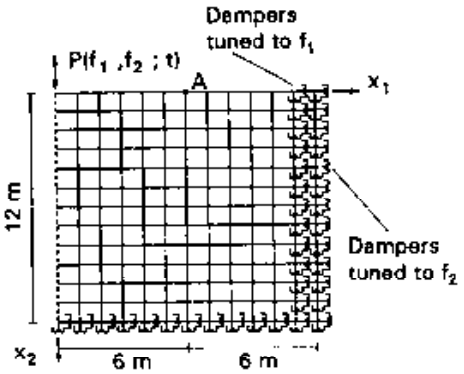

Fig. 10. (b) FEM modeling and discretization of semi-infinite soil media [11].

method, tends to be stiffer than the actual one. A considerable reduction of this error may be achieved by increasing the number of elements at the contact area. In Fig. 9, the percentage error in the numerical evaluation of the complex amplitude $|v_2(C)|$ obtained using the BEM–FEM as compared with that given by the analytical/numerical solution [1] is presented vs the number of boundary elements M_c for the rigid plate of Fig. 4 subjected to a vertical load at C. It is apparent that only a few elements are sufficient to obtain excellent results.

In the second example, the transient response of point A at the surface of the soil medium shown in Fig. 10a is evaluated using the frequency domain hybrid BEM–FEM approach. The results are compared with a strictly FEM solution of the same problem, given by Elmer *et al.* [11]. The soil is characterized by a modulus of elasticity $E_s = 10^5\,\text{kN/m}^2$, mass density $\rho_s = 2.0\,\text{kN/m}^3$ and Poisson's ratio $\nu_s = 0.4$. The soil surface is subjected to a vertical transient load that includes two frequencies only, namely $f_1 = 17.5$ Hz and $f_2 = 22.5$ Hz. Since the bulk of the strain energy in the soil is developed through Rayleigh waves, two series of dashpots tuned as suggested by Lysmer and Kuhlemeyer [10] are placed along the surface of the soil model, as illustrated in Fig. 10b. The final time-dependent response at point A, obtained by synthesis of the frequency components, is plotted in Fig. 11, and is almost identical to the one obtained by the pure FEM method [11]. The CPU time required to evaluate the response amplitude corresponding to the 17.5 Hz frequency was only 3.5 CPU min. The CPU time required for the FEM analysis of Elmer *et al.* is not

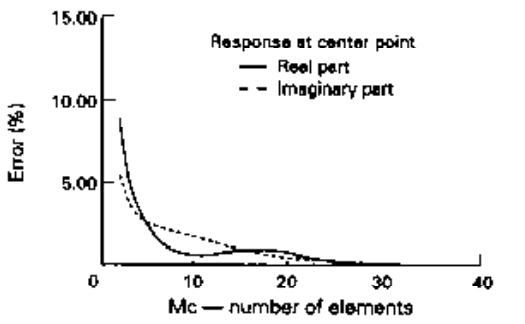

Fig. 9. Percent error in the vertical response of rigid plate subjected to vertical load.

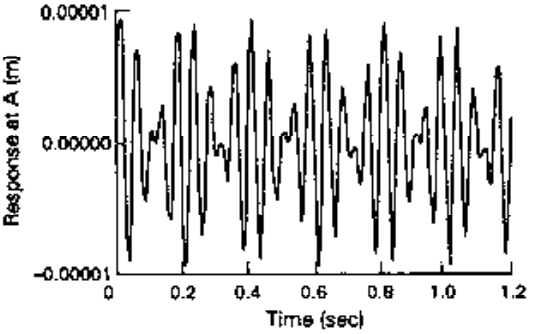

Fig. 11. Time-dependent response at point A obtained using the hybrid BEM–FEM method.

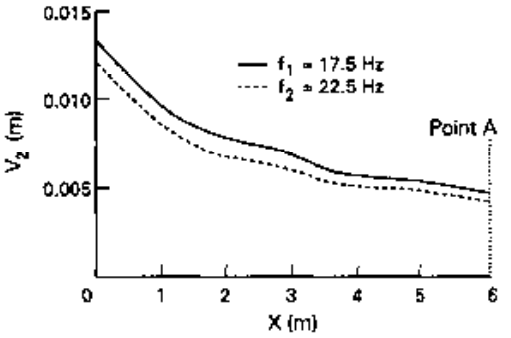

Fig. 12. Displacement profile for frequencies f_1 and f_2 of the exciting load.

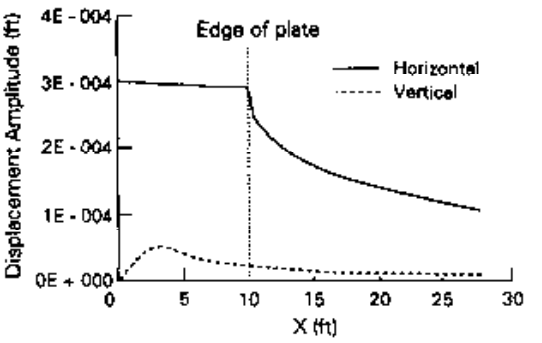

Fig. 14. Horizontal amplitudes for horizontal force. Vertical amplitudes for moment at C ($a_0 = 1$, $K_r = 0.05$, $M_r = 1.25$).

available to compare the efficiency of the two approaches. However, the CPU time required for the same analysis using the ANSYS program was 19.32 CPU min, which clearly indicates the advantage of BEM in solving dynamic SSI problems. Figure 12 portrays the soil displacement profile for the two frequencies f_1 and f_2. The displacements decrease with increasing value of the frequency f and both plots clearly show the decay of the response amplitudes due to radiation damping.

Consider a flexible strip-foundation being in contact with a homogeneous isotropic linear elastic half-space. The soil properties are taken as the modulus of elasticity $E_s = 3.2256 \times 10^6$ lb/in^2, Poisson's ratio $\nu_s = 0.4$, mass density $\rho_s = 3.75$ lb sec^2/ft^4 and damping coefficient $\zeta_s = 0.05$. The foundation under consideration has width $2b = 20$ ft, thickness $h = 0.5$ ft, Poisson's ratio $\nu_f = 0.2$ and damping coefficient $\zeta_f = 0.02$. The parameters characterizing the flexibility and inertia of the soil–foundation system are the relative stiffness and relative mass defined by

$$K_r = \frac{E_f h^3}{1 - \nu_f^2} \frac{1 + \nu_s}{E_s b^3}$$

and

$$M_r = \frac{\rho_f}{\rho_s},$$

respectively. The soil surface under the strip-foundation is discretized into 16 boundary elements and the free soil surface into four uneven elements at each side of the foundation. The response of the soil–foundation system is determined first for vertical load $P_2 = 1000$ lb acting at the center point C and having dimensionless frequency $a_0 = 1$. The vertical response amplitudes are obtained for representative values of the relative stiffness K_r and the relative mass M_r, and are given graphically in Fig. 13. The relative stiffness takes the values 0.05, 5 and 500, which correspond to flexible, intermediate and almost rigid strip-foundation, respectively, while the relative mass takes the values 1.25 and 4, which represent a concrete and a steel plate. It can be easily observed that the displacements increase as the foundation becomes more flexible and although the effect of different mass densities on the response is very small, the displacement of the soil–foundation system also increases, when the total mass of the plate increases. In Fig. 14, the variation of the horizontal and vertical displacement amplitudes along the soil surface are presented for horizontal force $P_1 = 1000$ lb and moment $M_3 = 1000$ lb ft, respectively.

The steady-state response of a rigid massive strip-foundation subjected to Rayleigh waves is studied. A modulus of elasticity $E_s = 1.24 \times 10^{11}$ N/m^2, Poisson's ratio $\nu_s = 0.25$ and mass density $\rho_s = 5362.45$ kg/m^3 are adopted as material properties of the supporting soil, while the strip-plate is characterized by a mass density $\rho_f = 7.5\,\rho_s$ and thickness $h = 0.2\,b$. The proposed hybrid BEM–FEM method is compared here with the time domain direct boundary element

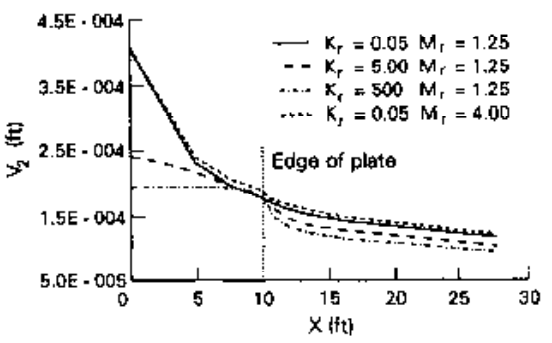

Fig. 13. Displacement profile for vertical load at the center of the flexible massive foundation ($a_0 = 1$).

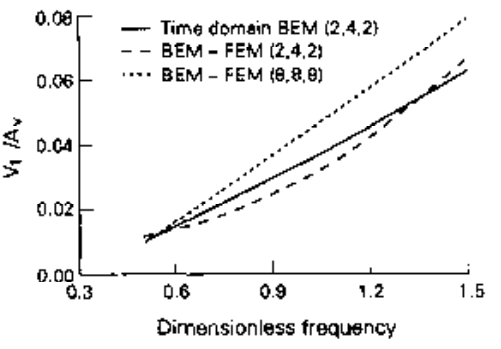

Fig. 15. Horizontal Rayleigh-wave response amplitude of massive rigid strip-foundation.

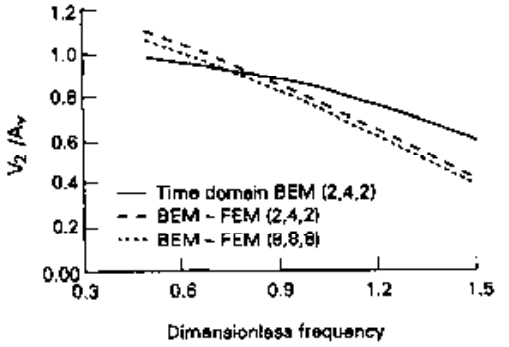

Fig. 16. Vertical Rayleigh-wave response amplitude of massive rigid strip-foundation.

method proposed by Antes and Spyrakos [22]. The results of the time domain BEM are transformed to the frequency domain through a Fast Fourier Transform. In order to analyze the response of the soil–foundation system, two discretization patterns have been considered. For the first one, which is suggested in [22], an amount of free surface equal to b is divided into two elements at each side of the plate, and the contact area is discretized into four boundary elements. For the second pattern, which was introduced to capture more accurately the free field displacement distribution along the soil surface, each part of the free surface has length $4b$ and is divided into eight elements, while the discretized contact surface consists of eight boundary elements. The response of the rigid massive block was obtained for the vertical component of the impulsive Rayleigh wave propagating along the x_1x_2-plane, with free field displacement amplitudes given by

$$u_2^f(\omega) = A_v e^{-i\omega x_1/c_R},$$

where ω is the frequency of the plane wave excitation and $c_R = 0.9194\ c_2$ the Rayleigh wave velocity. The difference in the results of the two methods is attributed to the fact that the time domain BEM is used to obtain the response of a massive rigid block and the surface foundation is considered as a limiting situation corresponding to a block with very small height compared with width. However, the results of both methods have the same trends and show clearly the effect of Rayleigh waves on the structural system.

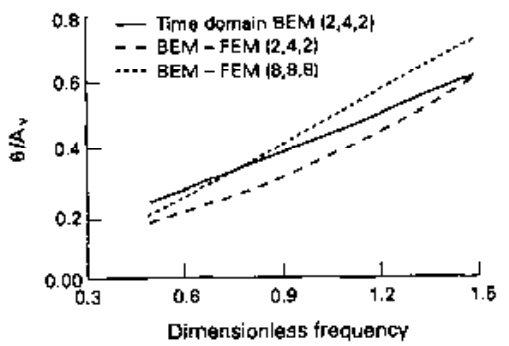

Fig. 17. Rotation of massive rigid strip-foundation subjected to Rayleigh waves.

4. CONCLUSIONS

A hybrid BEM–FEM method has been developed to study the dynamic behavior of flexible massive strip-foundations. In particular, two separate formulations are presented in order to investigate the cases of harmonic loads and seismic waves. The salient features of the BEM–FEM have been compared with approximations commonly adopted by analytical/numerical approaches or purely numerical FEM methods. Comparisons of the results have shown to be in a very good agreement with those given in the literature, even for a relatively small number of elements. They have also revealed that, in some cases, the hybrid method appeared to be more advantageous over other methods, since it provided a more realistic simulation of the physical problem. The frequency domain BEM–FEM approach has proven to be more efficient and considerably faster than time domain methods in analyzing soil structure interaction problems, involving a transient excitation with a small number of harmonic components. An important aspect that should be further investigated is the coupling conditions at the soil–foundation interface. The conditions adopted in this work are not very well refined and seem to lead to an increase of the overall stiffness of the system. This weakness of the formulation may be alleviated either by using a more dense discretization, which is not an efficient solution to the problem, or by incorporating into the coupling conditions the shape functions of the finite beam elements.

REFERENCES

1. G. Gazetas, Analysis of machine foundation vibrations: state of the art. *Soil Dyn. Earthquake Engng* **2**, 1–42 (1983).
2. P. K. Banerjee and R. Butterfield, *Boundary Element Methods in Engineering Sciences*. McGraw-Hill, London (1981).
3. T. A. Cruze and F. J. Rizzo, A direct formulation and numerical solution of the general transient elastodynamic problem—I. *Int. J. Math. Anal. Appl.* **22**, 244–259 (1968).
4. Y. Niwa, S. Kobayashi and T. Fukui, Applications of integral equation method to some geomechanical problems. In *Numerical Methods in Geomechanics* (Edited by C. S. Desai), pp. 120–131. ASCE, New York.
5. R. P. Banaugh and W. Goldsmith, Diffraction of steady elastic waves by surfaces of arbitrary shape. *J. appl. Mech.* **30**, 589–597 (1963).
6. M. Ottenstreuer and G. Schmid, Boundary elements applied to soil–foundation interaction. *Proceedings of 3rd International Seminar on Recent Advances in Boundary Element Methods* (Edited by C. A. Brebbia), Irvine CA, pp. 293–309. Springer, Berlin (1981).
7. H. Antes and v. O. Estorff, Dynamic soil–structure interaction by BEM in the time and frequency domain. 8th European Conference on Earthquake Engineering, Lisbon, Portugal (1986).

8. O. C. Zienkiewicz, *The Finite Element Method*, 3rd Edn. McGraw-Hill, New York (1977).
9. K. J. Bathe, *Finite Element Procedures in Engineering Analysis*. Prentice-Hall, Englewood Cliffs, New Jersey (1982).
10. J. Lysmer and R. L. Kuhlemeyer, Finite dynamic model for infinite media. *J. Engng Mech. ASCE* **4**, 859–877 (1969).
11. K. H. Elmer, H. G. Natke and R. Thiede, Modelling in soil dynamics by a finite domain with respect to transient excitation. *Proceedings of Earthquake Engineering Soil Dynamics*, Princeton, pp. 347–365 (1987).
12. J. P. Wolf, *Dynamic Soil–Structure Interaction*. Prentice-Hall, Englewood Cliffs, New Jersey.
13. C. C. Spyrakos, P. N. Patel and D. E. Beskos, Dynamic analysis of flexible embedded foundations: plane strain case. Proceedings of the 3rd International Convention on Computing Methods and Experimental Measures, Port Carras, Greece (1986).
14. A. P. Gaitanaros and D. L. Karabalis, Dynamic analysis of 3-D flexible embedded foundations by a frequency domain BEM–FEM. *Earthquake Engng Struct. Dynam* **16**, 653–674 (1988).
15. O. C. Zienkiewicz, D. W. Kelly and P. Bettess, The coupling of the finite element method and boundary solution procedures. *Int. J. Numer Meth. Engng* **11**, 355–375 (1977).
16. D. L. Karabalis and D. E. Beskos, Dynamic response of 3-D flexible foundations by time domain BEM and FEM. *Soil Dynam. Earthquake Engng* **4**, 91–101 (1985).
17. C. C. Spyrakos and D. E. Beskos, Dynamic response of flexible strip-foundations by boundary and finite elements. *Soil Dynam. Earthquake Engng* **5**, 84–96 (1986).
18. H. R. Riggs and G. Waas, Influence of foundation flexibility on soil–structure interaction. *Earthquake Engng Struct. Dynam.* **13**, 597–615 (1985).
19. H. L. Wong and J. E. Luco, Dynamic response of rectangular foundations in obliquely incident seismic waves. *Earthquake Engng Struct. Dynam.* **6**, 3–16 (1978).
20. W. L. Whittaker and P. Christiano, Response of a plate and elastic half-space to harmonic waves. *Earthquake Engng Struct. Dynam.* **10**, 255–266 (1982).
21. J. Dominguez, *Response of Embedded Foundations to Travelling Waves*. Publication No. R78-20, Department of Civil Engineering, M.I.T., Cambridge, MA.
22. H. Antes and C. C. Spyrakos, Dynamic response of massive block to transient Rayleigh waves. Proceedings of the ASCE Structures Congress, Volume on Dynamics of Structures (Edited by J. M. Roesset), pp. 512–518 (1987).
23. P. Hillmer and G. Schmid, Calculation of foundation uplift effects using a numerical Laplace transform. *Earthquake Engng Struct. Dynam.* **16**, 789–801 (1988).
24. T. A. Cruse, The transient problem in classical elastodynamics solved by integral equations. Ph.D. thesis, University of Washington (1967).
25. F. J. Rizzo and D. J. Shippy, An application of the correspondence principle of linear viscoelasticity theory. *SIAM J. appl. Math.* **2**, 321–330 (1971).
26. S. H. Crandall, The role of damping in vibration theory. *J. Sound Vibr.* **11**, 3–18 (1970).
27. F. T. Kokkinos, Hybrid BEM–FEM dynamic analysis of flexible strip-foundations. Master thesis, West Virginia University, Morgantown, WV, pp. 114–126 (1988).
28. M. Abramovitz and I. E. Stegun, *Handbook of Mathematical Functions*. National Bureau of Standards, Washington, D.C., pp. 374–480 (1965).
29. G. N. Watson, *A Treatise on the Theory of Bessel Functions*. Cambridge University Press, London.
30. C. C. Spyrakos and D. E. Beskos, Dynamic response of frameworks by fast Fourier transform. *Comput. Struct.* **15**, 495–505 (1982).
31. S. A. Thau, Radiation and scattering from a rigid inclusion in an elastic medium. *J. appl. Mech. ASME* **34**, 509–511 (1967).